

Gd₂O₂S:Eu³⁺ Nanophosphors: Microwave Synthesis and X-ray Imaging Detector Application

Sapizah Rahim^{a,b,*}, Muhammad Hassyakirin Hasim^a, Muhammad Taqiyuddin Mawardi Ayob^a,

Irman Abdul Rahman^a, Khairul Anuar Mohd Salleh^b, Shahidan Radiman^a

^aNuclear Technology Research Centre, Faculty Science and Technology, University Kebangsaan Malaysia, 43600, Bangi, Selangor, Malaysia

^bLeading Edge Non Destructive Testing Group (LENDT), Industrial Technology Division, Agensi Nuklear Malaysia, 47000, Kajang, Selangor, Malaysia

Received: June 17, 2019; Revised: November 17, 2019; Accepted: January 6, 2020

Red-emitting Gd₂O₂S:Eu³⁺ nanophosphors were successfully prepared using a microwave irradiation method followed by hydrogenation treatment. The optimum calcination temperature (900 °C) was determined by thermogravimetric-differential scanning calorimetry. The X-ray diffraction results showed that all the samples consisted of the pure hexagonal Gd₂O₂S:Eu³⁺ phase. The field emission scanning electron microscopy images showed that the Gd₂O₂S:Eu³⁺ nanophosphors were spherical, and their average particle diameter increased parallel with the microwave irradiation power. The photoluminescence spectra (under 325-nm excitation) of the samples exhibited red emission corresponding to the ⁵D₀→⁷F₂ transition of Eu³⁺ ions. A Gd₂O₂S:Eu³⁺ nanophosphor screen film was fabricated using the particle-binder sedimentation method. The result shows that the luminance of the Gd₂O₂S:Eu³⁺ nanophosphor screen film increased with an increase in the X-ray energy. Hence, this film would become one of the potential candidate for future imaging applications.

Keywords: Gd₂O₂S:Eu³⁺ nanophosphors, microwave, luminescent, imaging detector.

1. Introduction

Phosphors are well-known materials that exhibit luminescent phenomena when they absorb a certain amount of energy. Trivalent europium-activated gadolinium oxysulfide (Gd₂O₂S:Eu³⁺) nanophosphor is important luminescent material especially for imaging displays for medical and industrial applications¹. Gd₂O₂S:Tb³⁺ phosphors are widely used in conventional imaging detectors such as storage phosphors because of their strong green emitting². The rapid developments in imaging technologies make changed from conventional imaging to digital imaging, which uses amorphous silicon detectors. However, silicon detectors coupled with Gd₂O₂S:Tb³⁺ phosphors produce images with low sensitivity and poor definition³. This is because only 45 – 55 % of the light (λ:500-550 nm) generated by terbium activated phosphor will be detected by the silicon and CMOS devices incorporated in x-ray imaging systems due to less sensitive towards green light⁴. It is well known that silicon based photodetectors more sensitive to longer wavelength ranges and therefore, red-emitting Gd₂O₂S:Eu³⁺ nanophosphors should be of interest to investigate.

Nowadays, the improvement of luminescent materials used for imaging purposes and solid-state applications intensively investigated especially in preparation method. Various methods such as the conventional solid-state reaction⁵, combustion⁶, solvothermal⁷, hydrothermal⁸, sol-gel⁹, and precipitation¹⁰ methods have been reported for the synthesis of red-emitting Gd₂O₂S:Eu³⁺ nanophosphors. Most of these methods require high sintering temperatures, which effects the expansion of the crystalline lattice and lead to the mechanical instability¹¹ of the resulting nanophosphors.

However, a few reports were published using synthesized nanophosphor for digital imaging application with good emission efficiency by controlled synthesis process using surfactant or polymer¹². Therefore, microwave irradiation was used to synthesize Gd₂O₂S:Eu³⁺ in the presence of PVP because this method is quite advantageous as the synthesis process can be tuned to yield desired size and shape, as well as purity of nanoparticles¹³. Furthermore, the luminescence properties of phosphors are significantly affected by the particle scale and morphology. Surfactants or polymers were used as binders and protective agents to prevent particle aggregation and control the chemical reactions during microwave irradiation^{14,15}.

Apart from that, there are few studies have been carried out to investigate the effect of the particle size of nanophosphors on their luminescence efficiency to achieve better luminescence dynamics^{16,17}. Additionally, the quantum confinement and surface plasmon resonance phenomena of nanophosphors also been investigated^{18,19}. However, the surface quenching effect-induced luminescence dynamics of nanophosphors have not been elucidated especially for Gd₂O₂S:Eu³⁺ phosphors. Thus, this work reports the use of polyvinyl pyrrolidone (PVP) and ethylene glycol as a binder and protective agent in the preparation of red-emitting Gd₂O₂S:Eu³⁺ nanophosphors using microwave irradiation method. The effect of synthetic strategy such as microwave irradiation power and calcination temperature on the size, crystallinity and luminescence properties has been compared.

2. Experimental Procedure

Gadolinium (III) nitrate hexahydrate (Gd(NO₃)₃·6H₂O, 99.9%), europium (III) nitrate (Eu(NO₃)₃·5H₂O, 99.9%), and PVP (wt ~40000) were obtained from Sigma-Aldrich, USA.

*e-mail: sapizah@gmail.com

Ammonium sulfate ((NH₄)₂SO₄) and ethylene glycol were purchased from Merck. All the reagents were of analytical grade and were used as purchased without further purification. Deionized water (DI: 18 Ω) was used as the solvent for all the experiments.

Gd(NO₃)₃, Eu(NO₃)₃ and (NH₄)₂SO₄ were weighed in a suitable stoichiometric ratio and were dissolved in a 1:1 mixture of deionized water and ethylene glycol²⁰. 2% w/v of PVP was added to the reaction mixture and vigorous stirred for 2 h. The resulting mixture was then divided into four samples (control, 167, 500, and 1000 W) and microwave irradiated for 2 min. The irradiated samples were then cooled down to room temperature, centrifuged, and washed with ethanol and DI water several times. The solid precipitates obtained were dried overnight in air at 80 °C and calcined at 900 °C for 2 h under the flow of hydrogen gas. After that, the phosphor film was fabricated by adding 0.5 mg of Gd₂O₂S:Eu³⁺ powder to the binder solution (polyvinyl alcohol (5wt %), ethylene glycol (0.3 vol.%), and dioctyl sulfosuccinate sodium salt (0.3 vol.%) in 20 mL of DI water). The mixture was agitated for 2 h to avoid the agglomeration of PVA and phosphor. This solution was then transferred to a beaker with 1.0 cm x 1.0 cm polymer base substrates at the bottom overnight for sedimentation. The residue solution was removed and the phosphor film was dried at 60 °C for 2 h before further characterization

2.1 Characterization

The microwave radiation source used in this study was a conventional microwave oven (PANASONIC model) with a microwave frequency of 2450 MHz. Thermogravimetric-Differential scanning calorimetry (TG-DSC) analysis was carried out using a METTLER TOLEDO (TGA/SDTA 851e) integrated thermal analyzer over a temperature range of 25-1400 °C at a heating rate of 10 °C/min under the air flow. The X-ray diffraction (XRD) patterns of the Gd₂O₂S:Eu³⁺ nanophosphor samples were obtained using a Bruker X-ray diffractometer working in the reflection mode at 40 kV and 40 mA with Cu Kα radiation (λ = 0.15406 nm). The scanning rate (2θ: 20 - 80°) used for identifying the phase formation was 5 °/min. The morphology and size distribution of the samples were investigated by field emission scanning electron microscopy (FESEM-Carl Zeiss, Supra 35VP). Meanwhile, the photoluminescence (PL) spectra of the samples were recorded over the range of 300 - 800 nm using a FLSP920 Edinburgh spectrometer. The luminance properties of nanophosphor film were evaluated using X-ray machine (ISOVOLT Titan 220) at 10 mA and different energy (60, 80, 100, 120, 140, 160 and 180 kV), luxmeter, ±0.01 lx (Gossen) and lead (5 x 5 x 10 cm) as shielding.

3. Results and Discussion

The thermal behavior of the samples was investigated by carrying out a TG-DSC analysis (from room temperature to

1000 °C) (Figure 1). The optimum calcination temperature for the precursors was also determined using TG-DSC. Five distinct weight loss regions were observed over the entire temperature range (the total weight loss being ~43%), as shown in Figure 1(a). The weight loss at temperatures lower than 250 °C can be attributed to the evaporation of water molecules and organic residue²¹. The weight loss within the temperature range of 250–400 °C can be attributed to the dehydroxylation of the precursors, indicating the presence of hydroxyl groups²². The weight loss in these two regions can be associated with the weak endothermic DSC peaks at around 160 and 310 °C. The third weight loss region was observed between ~400 and ~650 °C. In this region, the samples showed a weight loss of about 15% (by mass) corresponding to the degradation of the CH₃COO groups from ethylene glycol and their oxidation to carboxylic acids¹¹. A continuous weight loss (18% by mass) was observed over the temperature range of 650–900 °C, attributed to the oxidation (exothermic reaction at ~950 °C) of the precursors and the crystallization of amorphous Gd₂(SO₄)₃ into crystalline Gd₂O₂SO₄ particles. Therefore, 900 °C was chosen as the final calcination temperature for the crystallization of

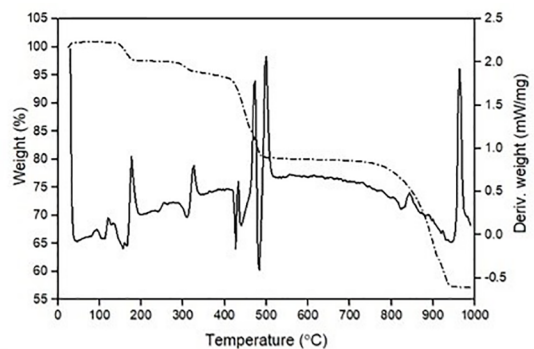


Figure 1. TG-DSC curves of the precursor (1000 W microwave irradiation power) from room temperature to 1000 °C.

Gd₂O₂SO₄ under the flow of hydrogen to form the Gd₂O₂S nanophosphors as in Eq.1²³:



The crystallinity behavior of the samples microwave irradiated at 1000 W and calcined at various temperatures (up to 900 °C) in the absence of hydrogen is shown in Figure 2(a). The sharp peaks have observed after calcining at 650 °C, indicating the transformation of the amorphous phase to a single crystalline phase²². The diffraction peaks could be indexed to the hexagonal Gd₂O₂SO₄:Eu³⁺ phase (JCPDS No: 01-077-9842). The oxygen molecules in the SO₄ groups of the samples were removed by calcining at 900 °C under the flow of hydrogen. As a result, well-defined diffraction peaks were observed for each microwave irradiation power as shown in Figure 2(b). These peaks could be indexed to the hexagonal Gd₂O₂S:Eu³⁺ phase (JCPDS No: 00-026-1422) with no impurity peaks were observed. Therefore, during the

microwave treatment, Eu³⁺ ions are effectively occupied the Gd³⁺ lattice without changing the host structure²². There is no shift in the peaks at different microwave irradiation power but slightly affected the intensity of the peaks demonstrate no changes in hexagonal phase. Furthermore, the peak intensity is dependence on the size and electron density of the Gd₂O₂S:Eu³⁺ particles²⁴.

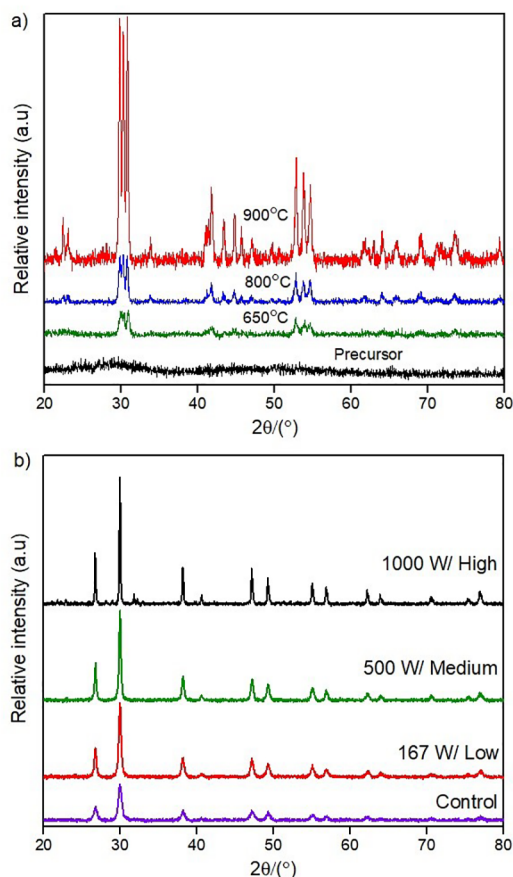


Figure 2. XRD patterns of a) the as-formed and calcined Gd₂O₂S:Eu³⁺ nanophosphors (650, 800, and 900 °C without hydrogen flow at 1000 W) and b) Gd₂O₂S:Eu³⁺ nanophosphors for control (without microwave irradiation) and at low (167 W), medium (500 W), and high (1000 W) microwave irradiation powers.

The FESEM images of the Gd₂O₂S:Eu³⁺ nanophosphors produced in this study are shown in Figure 3. The images revealed that these nanophosphors were mainly composed of spherical nanostructures. The samples showed a coral-like morphology due to particle agglomeration. The mean of single particle size of all the samples was found to be less than 200 nm (Figure 3e). The particles size of nanophosphor increased with increasing microwave irradiation power because the irradiation power will affect the surface energy and thermodynamically unstable during nucleation process. Therefore, the agglomeration process take place to minimize surface energy through van der Waals force interaction to form larger particles²⁵. This phenomenon can be attributed to Ostwald ripening or the growth of larger crystals from

those of smaller size through dissolution of smaller particles spontaneously in an attempt to decrease the total surface energy after nucleation process²⁶

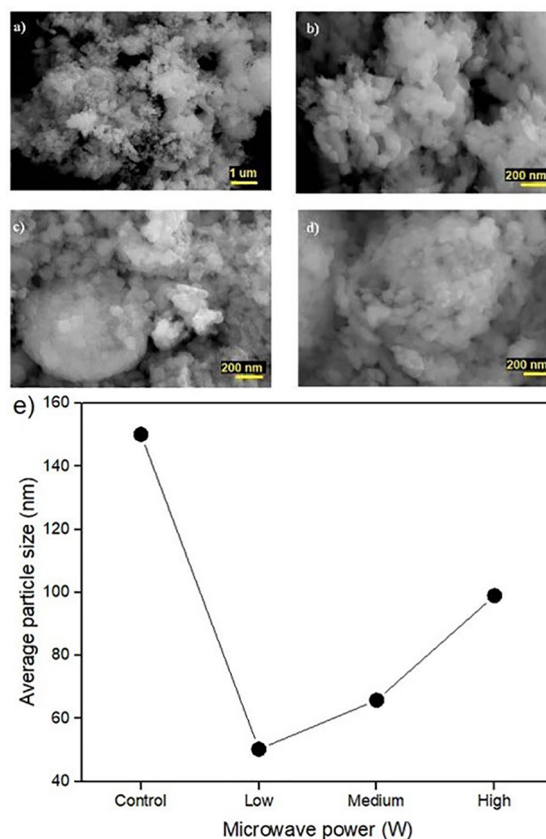


Figure 3. FESEM images of the red-emitting Gd₂O₂S:Eu³⁺ nanophosphors at a) control (without microwave) b) 167 W c) 500 W and d) 1000 W and e) the average size of the Gd₂O₂S:Eu³⁺ nanophosphors at different microwave powers.

Another reason is microwave irradiation could changes the thermal transfer of latent heat in the solution followed by dissipation by active-air cooling during the synthesis²⁷. Furthermore, this phenomenon can be related to the thermal agitation of liquid molecules, which causes surface enrichment during microwave irradiation²⁸. Therefore, during the nucleation process, PVP played an important role in the formation of spherical nanostructures. In aqueous solutions, ethylene glycol forms a stable Gd-OCH₂CH₂-OH complex and produces a colloidal sol through the hydrolysis reaction²⁹. PVP covered the precursor surface and formed a protective layer, controlling the growth rate of the precursor particles³⁰. Since the PVP concentration was high enough to be adsorbed on the surface of the particles in all the directions to entail an isotropic growth, stable spherical nanophosphors were obtained²⁰.

Figure 4a shows the photoluminescence spectra of the samples obtained under the excitation at 325 nm. All samples show strong red-emission peaks corresponding to the ⁵D₀ → ⁷F_j (j=0, 1, 2, 4) transitions³¹. The strongest red-emission

peak split into two peaks at 617 and 627 nm. These peaks correspond to the Stark splitting of the $^5D_0 \rightarrow ^7F_2$ transition in Eu^{3+} ions³². In PL emission process, trivalent Gd^{3+} ions, acted as the sensitizer, absorbed ultraviolet excitation, and transferred energy to the neighboring Eu^{3+} ions (as the activator), resulting in the overall red emission of Eu^{3+} ions³³. Figure 4(b) shows the emission spectra of the $\text{Gd}_2\text{O}_2\text{S}:\text{Eu}^{3+}$ nanophosphors at different microwave irradiation powers. While the microwave irradiation power were increased, the luminescent intensity of the nanophosphors also increased due to the surface quenching effect³⁴. The results obtained with 1000 W irradiation power are consistent with those obtained by Wang et al. (2007). They reported that with increasing of the microwave irradiation power, the PL intensity of $\text{Gd}_2\text{O}_2\text{S}:\text{Eu}^{3+}$ phosphors would increase because of their smooth and small surface areas per volume³⁵. Furthermore, we also found that the PL intensity obtained in this study was much higher than that obtained by Osseni et al. (2011) who prepared $\text{Gd}_2\text{O}_2\text{S}:\text{Eu}^{3+}$ phosphors for medical applications by precipitating carbonate precursors³⁶. Apart from that, we also improved the synthetically method by set up the optimum microwave irradiation power to get strong red-emitting $\text{Gd}_2\text{O}_2\text{S}:\text{Eu}^{3+}$ nanophosphors rather than study the precursor ratios that was done by Zhai et al. (2007)³⁷

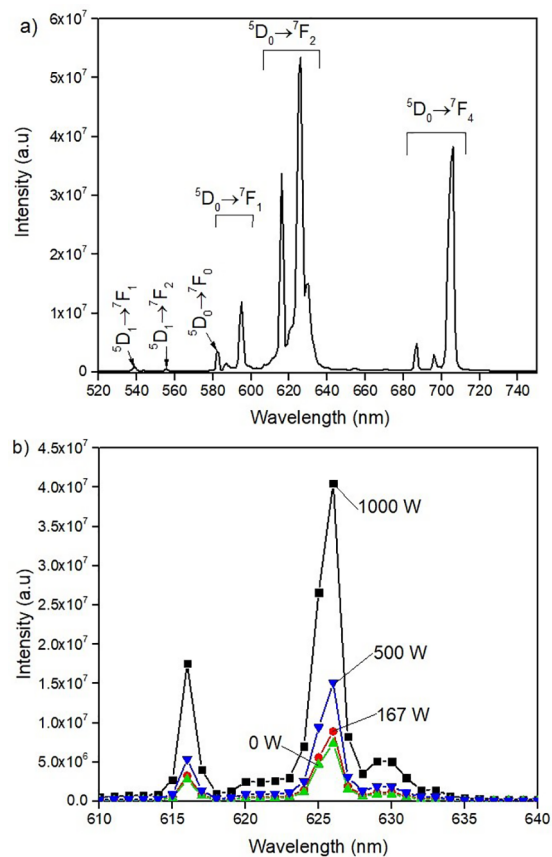


Figure 4. Photoluminescence emission ($\lambda_{\text{exc}}=325$ nm) of the red-emitting $\text{Gd}_2\text{O}_2\text{S}:\text{Eu}^{3+}$ nanophosphors a) corresponding to $^5D_0, 1 \rightarrow ^7F_j$ ($j=0, 1, 2, 4$) transition and b) at 0 W (no irradiation), 167 W (Low), 500 W (Medium) and 1000 W (High) microwave irradiation powers.

X-ray imaging detector application using $\text{Gd}_2\text{O}_2\text{S}:\text{Eu}^{3+}$ nanophosphors was done by systematically setup the instruments for measuring the light output as shown in Figure 5(a). The setup consisted of an X-ray source, a film, and a luxmeter connected to a computer. Lead block was used to protect the luxmeter from the ionizing radiation. The luminance of the $\text{Gd}_2\text{O}_2\text{S}:\text{Eu}^{3+}$ nanophosphor film at high microwave irradiation powers showed a linear relationship with the X-ray energy as shown in Figure 5(b). The luminance or brightness of the film increased with an increase in the electron energy because of the deeper penetration of phonons into the phosphor body³⁸. Therefore, the $\text{Gd}_2\text{O}_2\text{S}:\text{Eu}^{3+}$ nanophosphor film exhibited bright red luminescence under X-ray excitation. Hence, in our further study will be focus on film performance evaluation as this film is one of the potential candidate for imaging display devices.

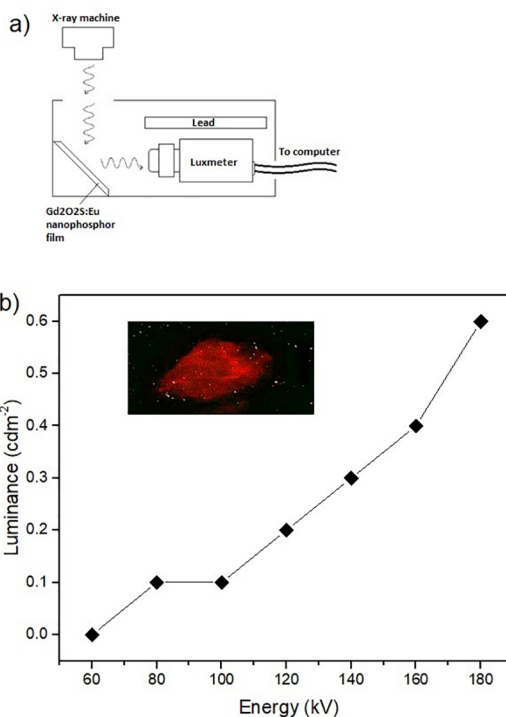


Figure 5. (a) Experimental setup for light output measurement and b) the light output of the $\text{Gd}_2\text{O}_2\text{S}:\text{Eu}$ nanophosphor film at 10 mA and 60, 80, 100, 120, 140, 160 and 180 kV (inset is film image under x-ray excitation).

4. Conclusion

We successfully prepared red-emitting $\text{Gd}_2\text{O}_2\text{S}:\text{Eu}^{3+}$ nanophosphors using a microwave irradiation method followed by hydrogenation. The properties of $\text{Gd}_2\text{O}_2\text{S}:\text{Eu}^{3+}$ nanophosphors were characterized and showed that all the samples consisted of the pure hexagonal $\text{Gd}_2\text{O}_2\text{S}:\text{Eu}^{3+}$ phase with spherical structure. Furthermore, the average particle diameter increased parallel with the microwave irradiation power. The photoluminescence spectra (under 325-nm excitation) of the samples exhibited red emission

corresponding to the ⁵D₀→⁷F₂ transition of Eu³⁺ ions. Simple particle-binder sedimentation method has used to fabricate screen film and the intensity of luminance was increased with an increase in the X-ray energy. Hence, microwave irradiation method can produced Gd₂O₃:Eu³⁺ nanophosphors and the fabricated screen film would become one of the potential candidates for future imaging applications.

5. Acknowledgement

This work was supported by the Ministry of Education (MOE), Malaysia (FRGS/1/2018/STG02/UKM/02/4 and GUP-2018-060) and Public Service Department of Malaysia.

6. References

- Wang F, Liu D, Yang B, Dai Y. Characteristics and synthesis mechanism of Gd₂O₃:Tb phosphors prepared by vacuum firing method. *Vacuum*. 2013;87:55-59.
- Park JK, Choi SR, Noh SC, Jung BJ, Choi IH, Kang SS. Fabrication and evaluation of a Gd₂O₃:Tb Phosphor screen film for development of a CMOS-Based X-ray imaging detector. *Journal for the Korean Physical Society*. 2014;65(3):351-354.
- Michail MC, Toutountzis A, Valais IG, Seferis I, Georgousis M, Fountos G, et al. Luminescence efficiency of Gd₂O₃:Eu powder phosphors as X-ray to light converter. *e-Journal Science and Technology*. 2010;25-32.
- Michail CM, Fountos GP, Liaparinos PF, Kalyvas NE, Valais I, Kandarakis IS, et al. Light emission efficiency and imaging performance of Gd₂O₃:Eu powder scintillator under X-ray radiography conditions. *Medical Physics*. 2010;37(7):3694-3703.
- Upadhyay K, Tamrakar RK, Dubey V. High temperature solid state synthesis and photoluminescence behavior of Eu³⁺ doped GdAlO₃ nanophosphor. *Superlattices and Microstructures*. 2015;78:116-124.
- Pawade VB, Swart HC, Dhoble SJ. Review of rare earth activated blue emission phosphors prepared by combustion synthesis. *Renewable and Sustainable Energy Reviews*. 2015;52:596-612.
- Das S, Som S, Yang CY, Lu CH. Optical temperature sensing properties of SnO₂:Eu³⁺ microspheres prepared via the microwave assisted solvothermal process. *Materials Research Bulletin*. 2018;97:101-108.
- Li Z, Wang Y, Cao J, Jiang Y, Zhao X, Meng, Z. Hydrothermal synthesis and luminescent properties of BaMoO₄:Sm³⁺ red phosphor. *Journal of Rare Earths*. 2016;34(2):143-147.
- Wang N, Liu Z, Tong H, Zhang X, Bai Z. Preparation of Gd₂O₃:Yb³⁺, Er³⁺, Tm³⁺ sub-micro phosphors by sulfurization of the oxides derived from sol-gel method and the upconversion luminescence properties. *Materials Research Express*. 2017;4(7):076205.
- Khachatourian AM, Fard FG, Sarpoolaky H, Vogt C, Vasileva E, Mensi M, et al. Microwave synthesis of Y₂O₃:Eu³⁺ nanophosphors: a study on the influence of dopant concentration and calcination temperature on structural and photoluminescence properties. *Journal of Luminescence*. 2016;169(Pt A):1-8.
- Gondolini A, Mercadelli E, Sanson A, Albonetti S, Doubova L, Boldrini S. Effects of the microwave heating on the properties of gadolinium-doped cerium oxide prepared by polyol method. *Journal of the European Ceramic Society*. 2013;33(1):67-77.
- Seferis IE, Kalyvas NI, Valais IG, Michail CM, Liaparinos PF, Fountos GP, et al. Light emission efficiency of Lu₂O₃:Eu nanophosphor scintillating screen under X-ray radiographic conditions. *Journal of Luminescence*. 2014;151:229-234.
- Moura AP, Oliveira LH, Nogueira IC, Pereira PFS, Li MS, Longo E, et al. Synthesis, structural and photophysical properties of Gd₂O₃:Eu³⁺ nanostructures prepared by a microwave sintering process. *Advances in Chemical Engineering and Science*. 2014;4(3):374-388.
- Gasaymeh SS, Radiman S, Heng LY, Saion E, Saeed GHM, Selangor B, et al. Synthesis and characterization of silver/polyvinylpyrrolidone (Ag/PVP) nanoparticles using gamma irradiation techniques. *American Journal of Applied Science*. 2010;7(7):892-901.
- Wilson GJ, Matijasevich AS, Mitchell DRG, Schulz JC, Will GD. Modification of TiO₂ for enhanced surface properties: finite ostwald ripening by a microwave hydrothermal process. *Langmuir*. 2006;22(5):2016-2027.
- Seferis IE, Zeler J, Michail C, David S, Valais I, Fountos G, et al. Grains size and shape dependence of light efficiency of Lu₂O₃:Eu thin screens. *Results in Physics*. 2017;7:980-981.
- Jain A, Hirata GA. Photoluminescence, size and morphology of red-emitting Gd₂O₃:Eu³⁺ nanophosphor synthesized by various methods. *Ceramics International*. 2016;42(5):6428-6435.
- Soo YL, Huang SW, Ming ZH, Kao YH, Smith GC, Goldburt E, et al. X-ray excited luminescence and local structures in Tb-doped Y₂O₃ nanocrystals. *Journal of Applied Physics*. 1998;83(10):5404-5409.
- Mohamed MB, Abouzeid KM, Abdelsayed V, Aljarash AA, El-Shall MS. Growth mechanism of anisotropic gold nanocrystals via microwave synthesis: formation of dioleamide by gold nanocatalysis. *ACS Nano*. 2010;4(5):2766-2772.
- Hasim MH, Rahman IA, Rahim S, Ayob MTM, Sharin S, Radiman S. Study the effect of γ -irradiation on gadolinium oxysulfide nanophosphors (Gd₂O₃S-NPs). *Journal of Nanomaterials*. 2017;2017:1-6.
- Nadagouda MN, Varma RS. Microwave-assisted synthesis of crosslinked poly(vinyl alcohol) nanocomposites comprising single-walled carbon nanotubes, multi-walled carbon nanotubes, and buckminsterfullerene. *Macromolecular Rapid Communications*. 2007;28(7):842-847.
- Lian J, Sun X, Liu Z, Yu J, Li X. Synthesis and optical properties of (Gd^{1-x},Eu^x)₂O₃SO₄ nano-phosphors by a novel co-precipitation method. *Materials Research Bulletin*. 2009;44(9):1822-1827.
- Lian J, Liu F, Zhang J, Yang Y, Wang X, Zhang Z, et al. Template-free hydrothermal synthesis of Gd₂O₃SO₄:Eu³⁺ hollow spheres based on urea-ammonium sulfate (UAS) system. *Optik*. 2016;127(20):8621-8628.
- Jensen H, Pedersen JH, Jorgensen JE, Pedersen JS, Joensen KD, Iversen SB, et al. Determination of size distributions in nanosized powders by TEM, XRD, and SAXS. *Journal of Experimental Nanoscience*. 2006;1(3):355-373.

25. Sanosh KP, Balakrishnan A, Francis L, Kim TN. Sol-gel synthesis of forsterite nanopowders with narrow particle size distribution. *Journal of Alloys and Compounds*. 2010;495(1):113-115.
26. Paula AJ, Parra R, Zaghete MA, Varela JA. Synthesis of KNbO_3 nanostructures by a microwave assisted hydrothermal method. *Materials Letters*. 2008;62(17-18):2581-2584.
27. Gerbec JA, Magana D, Washington A, Strouse GF. Microwave-enhanced reaction rates for nanoparticle synthesis. *Journal of the American Chemical Society*. 2005;127(45):15791-15800.
28. Phoempoon P, Sikong L. Phase transformation of VO_2 nanoparticles assisted by microwave heating. *Scientific World Journal*. 2014;2014:841418.
29. Song Y, You H, Huang Y, Yang M, Zheng Y, Zhang L, et al. Highly uniform and monodisperse $\text{Gd}_2\text{O}_2\text{S}:\text{Ln}^{3+}$ (Ln = Eu, Tb) submicrospheres: solvothermal synthesis and luminescence properties. *Inorganic Chemistry*. 2010;49(24):11499-11504.
30. Rahim S, Hasim MH, Ayob MTM, Rahman A, Radiman S. Gamma irradiation induced method in preparation of $\text{Gd}_2\text{O}_2\text{S}:\text{Eu}^{3+}$ phosphors: the effect of dose towards luminescent properties. *IOP Conference Series: Materials Science and Engineering*. 2018;298:1-4.
31. Lian J, Liu F, Liang P, Ren J. Synthesis of $\text{Gd}_2\text{O}_2\text{S}:\text{Eu}^{3+}$ hollow sphere by a hydrothermal method assisting with reduction route. *Journal of Ceramic Processing Research*. 2016;17(7):752-757.
32. Dhanaraj J, Jagannathan R, Kutty TRN, Lu CH. Photoluminescence characteristics of $\text{Y}_2\text{O}_3:\text{Eu}^{3+}$ nanophosphors prepared using sol-gel thermolysis. *Journal of Physical Chemistry: B*. 2001;105(45):11098-11105.
33. Huang J, Song Y, Sheng Y, Zheng K, Li H, Zhang H, et al. $\text{Gd}_2\text{O}_2\text{S}:\text{Eu}^{3+}$ and $\text{Gd}_2\text{O}_2\text{S}:\text{Eu}^{3+}/\text{Gd}_2\text{O}_2\text{S}$ hollow microspheres: solvothermal preparation and luminescence properties. *Journal of Alloys and Compounds*. 2012;532:34-40.
34. Wang F, Wang J, Liu XG. Direct evidence of a surface quenching effect on size-dependent luminescence of upconversion nanoparticles. *Angewandte Chemie International Edition*. 2010;49(41):7456-60.
35. Wang WN, Widiyastuti W, Ogi T, Lenggono IW, Okuyama K. Correlations between crystallite/particle size and photoluminescence properties of submicrometer phosphors. *Chemistry of Materials*. 2007;19(7):1723-1730.
36. Osseni SA, Lechevallier S, Verelst M, Dujardin C, Dexpert-Ghys J, Neumeyer D, et al. New nanoplatform based on $\text{Gd}_2\text{O}_2\text{S}:\text{Eu}^{3+}$ core: synthesis, characterization and use for in vitro bio-labelling. *Journal of Materials Chemistry*. 2011;21:18365-18372.
37. Zhai Y, Lui Y, Meng Y, Zhang S. Synthesis of the red long afterglow phosphor $\text{Gd}_2\text{O}_2\text{S}:\text{Eu}$, Mg, Ti by microwave radiation method and its luminescent properties. *Guang Pu*. 2007;27(4):634-638.
38. Wang T, Xu X, Zhou D, Qiu J, Yu X. Luminescent properties of $\text{SrGeO}_3:\text{Eu}^{3+}$ red emitting phosphors for field emission displays. *ECS Journal of Solid State Science and Technology*. 2014;3(8):R139-R143.